REPORT DOCUMENTATION PAGE

Form Approved
OMB No. 0704-0188

1. AGENCY USE ONLY (*Leave Blank*)

2. REPORT DATE
15 Sept 98

3. REPORT TYPE AND DATES COVERED
Final 97 Sept 01 - 98 May 31

4. TITLE AND SUBTITLE
High Frequency Electromagnetic Propagation/Scattering Codes

5. FUNDING NUMBERS
F49620-97-C-0070

6. AUTHOR(S)
Dr. Vladimir Oliker
Dr. Bjorn Engquist
Dr. Stanley Osher

AFRL-SR-BL-TR-98-
0701

7. PERFORMING ORGANIZATION NAME(S) AND ADDRESS(ES)
Matis, Inc.
1565 Adelia Place,
Atlanta, Georgia 30329

STTR-PH1

9. SPONSORING/MONITORING AGENCY NAME(S) AND ADDRESS(ES)
Air Force Office of Scientific Research
110 Duncan Avenue, Suite B115
Bolling AFB DC 20332-0001

10. SPONSORING/MONITORING AGENCY REPORT NUMBER

11. SUPPLEMENTARY NOTES
AFOSR Project Technical Monitor: Dr. Arje Nachman

12a. DISTRIBUTION/AVAILABILITY STATEMENT
No restrictions

DISTRIBUTION STATEMENT A
Approved for public release;
Distribution Unlimited

12b. DISTRIBUTION CODE

13. ABSTRACT (*Maximum 200 words*)
Two directions of work have been pursued. The first direction is concerned woth extensions and generalizations of geometric techniques for spatial and surface ray tracing and applications of these techniques to problems in high-frequency electromagnetics. The second direction is concerned with development of generalized eikonal and transport equations which can represent multiphase solutions and diffraction effects.

14. SUBJECT TERMS
Electromagnetics, Diffraction, Numerics

15. NUMBER OF PAGES
14

16. PRICE CODE

17. SECURITY CLASSIFICATION OF REPORT

18. SECURITY CLASSIFICATION OF THIS PAGE

19. SECURITY CLASSIFICATION OF ABSTRACT

20. LIMITATION OF ABSTRACT
SAR

MATIS, INC.

1565 Adelia Place, Atlanta, Georgia 30329 Tel. (404) 248-9926 Fax. (404) 248-0154

High Frequency Electromagnetic Propagation/Scattering Codes

Phase I - Final Technical Report

AFOSR STTR Contract F49620-97-C-0070
Contract Duration: 01 September 97 - May 31, 1998

Submitted by

Matis, Inc., 1565 Adelia Pl., Atlanta, Georgia 30329
tel. (404) 248-9926, fax (404) 248-0154
e-mail: matis@netcom.com

Principal Investigators:

Dr. Vladimir Oliker,	Matis, Inc.,
Dr. Bjorn Engquist,	UCLA,
Dr. Stanley Osher,	UCLA

September 15, 1998

Preface

The work presented in this report was performed at Matis, Inc., 1565 Adelia Place. Atlanta. Georgia 30329 and at UCLA, Department of Mathematics, University of California. Los Angeles, CA 90095-1555. Matis, Inc. served as the Prime Contractor and UCLA as the Sub-Contractor. This work was sponsored by the Air Force Office of Scientific Research under STTR Program. Period of performance September 1, 1997 - May 31, 1998. The project Technical Monitor was Dr. Arje Nachman from the AFOSR.

Contents

List of Figures

1 Introduction

Two directions of work have been pursued under this effort. The first direction is concerned with further extensions of our geometric techniques for spatial and surface ray tracing and applications of these techniques to problems in high-frequency electromagnetics. The second direction is concerned with development of generalized eikonal and transport equations which can represent multiphase solutions and diffraction effects. The first approach uses direct variational and geometrical methods for building numerically high-frequency solutions accounting for diffraction effects. It is applicable to geometrically complex objects, such as aircraft, ships, satellites, etc. The second approach is based on solving numerically the generalized eikonal and transport equations and has the capabilities to capture the behavior of solutions near caustic regions where multiphase solutions may develop.

The results obtained so far have shown that both directions of work lead to interesting theoretical results and numerical codes with capabilities for solving important and difficult high-frequency wave propagation problems. The two approaches are complementary to each other, and together they cover a large variety of problems in electromagnetics.

We describe now the results in more detail.

2 Calculation of geometric quantities required for computing currents and fields due to creeping waves

The work on this task involved five parts:

1. Investigation of efficient means for estimating the required length of continuation of geodesics into shadow region
2. Development of fast methods for determining shadow boundaries suitable for UTD calculations
3. Testing the accuracy of the algorithm for identifying the shadow boundary on aircraft models
4. Upgrading and testing of the algorithm and code for calculating the radii of curvature on faceted surfaces
5. Upgrading and testing of the algorithm and code for building initial approximations to geodesics.

In order to calculate currents in the shadow region one needs to construct the geodesics emanating from the shadow boundary into the shadow region. Our methods for computing geodesics on faceted surfaces are very fast. In particular, the number of operations required to calculate a single geodesic of length not exceeding the intrinsic diameter of the surface is at most of order O(N), where N is the number of facets. Usually, however, this estimate is overly pessimistic and the actual calculation of a geodesic requires processing of only a small fraction of of facets, therefore reducing significantly the computational time.

In certain cases, important for electromagnetic calculations, one needs to determine either a portion or an entire wavefront of a creeping wave produced by a source on the surface or in space. In such cases the wavefront can be a complicated set of points on the surface. An accurate determination of this wavefront may require tracing a dense set of geodesics emanating from the source and the issue of computational time may become critical. Typically, creeping wavefronts must be computed in situations when one needs to calculate currents produced by incident waves penetrating into the shadow region. In these cases a way of reducing the computational time needed to determine the required geodesics is to construct only the parts of geodesics on which the fields are above a certain significant level. This is based on the fact that, according to the results by V. A. Fock and other authors, the field intensity decays as the wave propagates into the shadow region. Therefore, it is desirable to have a criteria for terminating a geodesic once the field intensity is below some critical value. Application of such a criteria will allow to save on the computational time required for construction of geodesics.

We investigated this approach by using the numerical values of the Fock integral as the required criteria. We have developed an algorithm and code for calculating the Fock integral along an arbitrary surface geodesic. The implemented version requires that the surface file be represented as a collection of flat triangular facets. However, the algorithm is quite general and can be implemented with other surface representations, in particular, for surfaces represented by Nonuniform Rational Bi-cubic Splines (NURBS). Computationally, the evaluation of the Fock integral is fast and the results obtained so far show that the proposed way of dealing with this issue is satisfactory.

Another necessary step in computing currents and fields due to creeping waves is the determination of the shadow boundary. The shadow boundary has to be identified in two cases: (a) the source (or the field point) is at infinity and (b) the source (or the field point) is at a finite distance from the surface. For the case (a) we developed a very fast (of order $\log N$, where N is the number of facets in a surface) algorithm that determines the shadow boundary (boundaries) on an arbitrary flat-faceted surface. The algorithm is based on a "spreading spot" strategy. In this approach we pick first an arbitrary facet (call it F) and check the visibility condition for this facet. If the facet F is "visible" to the source, the program checks the neighboring facets for visibility and, if visible, adds them to the list of visible facets. Once all the neighboring facets of F are examined, the facet F is marked and not examined any more. Then all the neighboring facets of F are processed in the same fashion. This process continues until all facets that are visible to the source and can be

linked with F through a chain of visible facets are found.

If the facet F is invisible to the source, we build in the same way as before a collection of facets not visible to the source. As a result of this procedure the entire surface is divided into the lit and shadow regions. The boundaries of this regions are the required shadow boundaries.

This algorithm has been coded and tested on various surfaces, including aircraft models such as VFY218, Global Hawk, KC135, and F15. The code showed good performance and for canonical surface, such as spheres, ellipsoids, paraboloids, etc., the computed results were in agreement with results that can be predicted by analytic techniques.

It should be noted that at this stage this algorithm does not identify the occluded parts of a surface and therefore a part of the surface that is "blocked" from the source by another part of the surface will still be identified as visible. However, in many practical electromagnetic problems the results that can be computed with the already developed algorithm are sufficient.

In the case (b) when the source (or the field point) is at a finite distance from the surface only a minor modification of the algorithm is required to identify the shadow boundaries. This modification and the coding have been implemented and tested.

The next step consists in constructing a sufficiently dense set of surface geodesics that originate on the shadow boundary and penetrate into the shadow region. The distances by which these geodesics are continued into the shadow region are determined according to the criteria based on the values of the Fock integral as described earlier. The actual construction of the geodesics is done with the use of an algorithm that we developed earlier. The only modification that is needed here is to organize the calculations of geodesics in a way suitable for dealing with many "source" points located on the shadow boundary. The issue of positioning these equivalent sources on the shadow boundary is delicate because the shadow boundary may (and usually will) have a complicated geometry. We are working currently on this task. We tested the algorithm for identifying the shadow boundary as required for high frequency calculations. The results are satisfactory but more work is needed in order to improve the accuracy. The difficulties are connected with the fact that the typical aircraft geometry is quite complex and the usual acceleration strategies needed for fast computation of the shadow boundary rely on certain trade-offs that impact the accuracy. We are continuing working on this issue.

Several improvements have been made to our original code for computing radii of curvature of surface curves on faceted surfaces. These improvements enhance the accuracy of the calculations. We have also implemented a version of the Dijkstra algorithm for computing initial approximations to surface geodesics. The Dijkstra algorithm is a very efficient way for computing paths on faceted surfaces that pass through surface vertices. In our scheme,

the output of the Dijkstra algorithm provides initial approximations that are fed into our optimization code that determines the actual geodesics. Previously, in order to find the required initial approximations we used a specially developed projection algorithm. While the Dijkstra algorithm is more robust than our projection algorithm, it does not always capture all of the required geodesics. Consequently, we are using now a combined scheme in which both, our original projection algorithm and the Dijkstra algorithm are employed. The results are quite satisfactory in terms of robustness and accuracy.

3 Calculation of high frequency asymptotic expansions

We have used the FDTD technique applied to some simple geometries in order to validate the methods developed in this project. The codes for the FDTD simulation have earlier been developed in two and three space dimensions. They have now been adjusted to be useful for validation.

We have concentrated on the development of generalized eikonal equations. Two types of generalizations have been studied. One is the derivation of partial differential equations which can represent multiphase solutions. These solutions correspond to crossing rays. The other is the inclusion of diffraction effects.

The multiphase technique has now been extended to the time periodic case. This allows for the possibility of representing more crossing rays and gives a computationally faster algorithm. This method does not represent diffraction phenomena but gives a way to compute the ray paths.

The equations which include diffraction effects are of Schroedinger equation type. They give very good representation of diffraction phenomena and crossing rays as long as the angles between the rays are small. We have developed a robust numerical method.

We obtained a new set of partial differential equations (PDEs) which can be seen as a generalization of the classical eikonal and transport equations, to allow for solutions with multiple phases. The traditional geometrical optics pair of equations suffer from the fact that the class of physical relevant solutions is limited. In particular, it does not include solutions with multiple phases, corresponding to crossing waves. Our objective has been to generalize these equations to accommodate solutions containing more than one phase. The new equations are based on the same high frequency approximation of the scalar wave equation as the eikonal and the transport equations. However, they also incorporate a finite superposition principle. The maximum allowed number of intersecting waves in the solution can be chosen arbitrarily, but a higher number means that a larger system of PDEs must be

solved. The PDEs form a hyperbolic system of conservation laws with source terms.

Although the equations are only weakly hyperbolic, and thus not well-posed in the strong sense, several examples show the viability of solving the equations numerically. The technique we use to capture multivalued solutions is based on a closure assumption for a system of equations representing the moments.

In this contract we thus developed a middle way between geometrical optics and the kinetic model. It is a high-frequency approximation through which the whole field can be solved. Moreover, the superposition principle holds up to a point; the maximum allowed number of intersecting waves can be chosen arbitrarily, but a higher number means that a larger system of PDEs must be solved.

The starting point for this approach is the transport equation. Instead of solving the full equation in phase space. we observe that when f is of a simple form in $\mathbf{p}$. we can transform (1) to a finite system of moment equations in the reduced space (x, t). analogously to the classical approach of the hydrodynamic limit from a kinetic formulation.

$$f_t + v \cdot \nabla_x f + c\ \nabla_x n \cdot \nabla_p f = 0 \tag{1}$$

In particular, we are interested in cases where, for given x and t, the density function f is nonzero only for a finite number of p. This corresponds to a finite number of rays in different directions at each point.

The moment equations are derived from the kinetic model for high-frequency waves. They are equivalent to the equations of geometrical optics. We also explored some theoretical issues and find that the resulting hyperbolic equations are not well-posed in the strong sense. Existence of solutions of unbounded variation is indicated. Next, we solved these equations for one and two phases. The standard Lax-Friedrichs method gives satisfactory results. Most elaborate. and less viscous, methods like the Godunov method and the second-order TVD Nessyahu-Tadmor scheme, although converging well in L_1, suffer from problems locally and converge poorly in L_∞. For the two-phase system, the sensitivity of the equations is more pronounced and consequently it is harder to find stable numerical methods. After proper initialization. the equations can however be solved with the Lax-Friedrichs method.

The research on multiphase eikonal equations has continued by testing new closure assumptions.

The original closure assumption for the system of moment equations was a finite sum of delta functions in the space of ray directions. That means we assumed not more than a finite number of rays at each point in space. The new assumption is instead a finite sum of characteristic functions for intervals. The endpoints for the intervals correspond to rays in the geometrical optics approximation.

The advantage of the new assumption is that the final system of conservation laws only describes the ray pattern and not the amplitudes. It appears that this system will be more robust at caustics. A working code for this has been tested for 3 superimposed phases and is available upon request.

In addition, the FDTD research has continued in two directions. The parallelization of the code has been improved and tested on SMP nodes. The bandwidth to memory gives the limitations in the computations. A version of the code is available upon request.

In order to be able to simulate the electromagnetic field near small geometric details a new technique for wavelet compression of the difference operators has been tested for the Helmholtz equation. Before the compression the difference approximation describes the geometry in detail on a refined grid. The compression results in a coarser grid method which still approximates the fine geometric details.

This is part of work involving a systematic technique for the derivation of subgrid scale models in the numerical solution of partial differential equations. The technique is based on Haar wavelet projections of the discrete operator followed by a sparse approximation. As numerical testing suggests, the resulting numerical method will accurately represent subgrid scale phenomena on a coarse grid. Applications to wave propagation in materials with subgrid inhomogeneities are demonstrated below.

We consider the Helmholtz equation,

$$-\sum_{i=1}^{d} \frac{\partial}{\partial x_i}\left(a(x)\frac{\partial u}{\partial x_i}\right) - k^2 u(x) = 0. \tag{2}$$

for $a(x) > 0$.

We discretize (2) in one dimension, with the boundary conditions $u(0) = 1$ and $u'(1) = 0$.

$$\begin{aligned} -\frac{1}{h^2}\Delta_+ a_i \Delta_- u_i - k^2 u_i \quad 0. \quad & i = 1, \ldots, n, \\ u_0 &= 2u(0) - u_1, \\ u_{n+1} &= u_n. \end{aligned} \tag{3}$$

We use $k = 2\pi$ and $a(x) = \left\{ \frac{1}{6} \right.$ if $0.45 < x < 0.551$ otherwise and we take $n = 256$ and use three homogenizations. We get

$$\bar{L}_j u = (\hat{L}_j - k^2 I)u = 0. \tag{4}$$

Truncation is performed on $\hat{L}_j$ (or $\hat{H}_j$) and not on $\bar{L}_j$. The result is shown in Figure 1. We see that Helmholtz equation gives results similar to those of the model equation. Band

projection is more efficient than truncation and working on H_j the subgrid model, is more efficient than working on $\bar{L}_j$, the Schur complement.

We consider the two-dimensional version of (2) with periodic boundary conditions in the y-direction, and $u(0,y) = 1$, $u_x(1,y) = 0$ at the left and right boundaries respectively. This corresponds to a plane time-harmonic wave of amplitude one entering the computational domain from the left and flowing out at the right. The discretization that we use is

$$\begin{aligned} -\frac{1}{h^2}\Delta_+^x a_{i\ell}\Delta_-^x u_{i\ell} - k^2 u_{i\ell} &= 0, \qquad i,\ell = 1,\dots,n \\ u_{i,0} &= u_{i,n}, \\ u_{i,n+1} &= u_{i,1}, \\ u_{n+1,\ell} &= u_{n,\ell} \\ u_{0,\ell} &= 2 - u_{1,\ell}. \end{aligned} \tag{5}$$

This leads to the matrix equation

$$L_{j+1}U = F, \qquad U, F \in V_{j+1}, \qquad n = m2^{j+1}, \tag{6}$$

where m is a positive integer and L_{j+1} is homogenized following our theory for two-dimensional problems.

As an example we choose the $a(x,y)$ shown in Figure 2, which models a wall with a small slit where the incoming wave can pass through. With $k = 3\pi$ and $n = 48$, we obtained the results presented in Figure 3.

The structure of the operator after one homogenization step is shown in Figure 4. Truncation of this operator according to (5)-(6) gives the result shown in Figure 5 for various values of ν. The case $\nu = 9$ corresponds to a compression to approximately 7% of the original size.

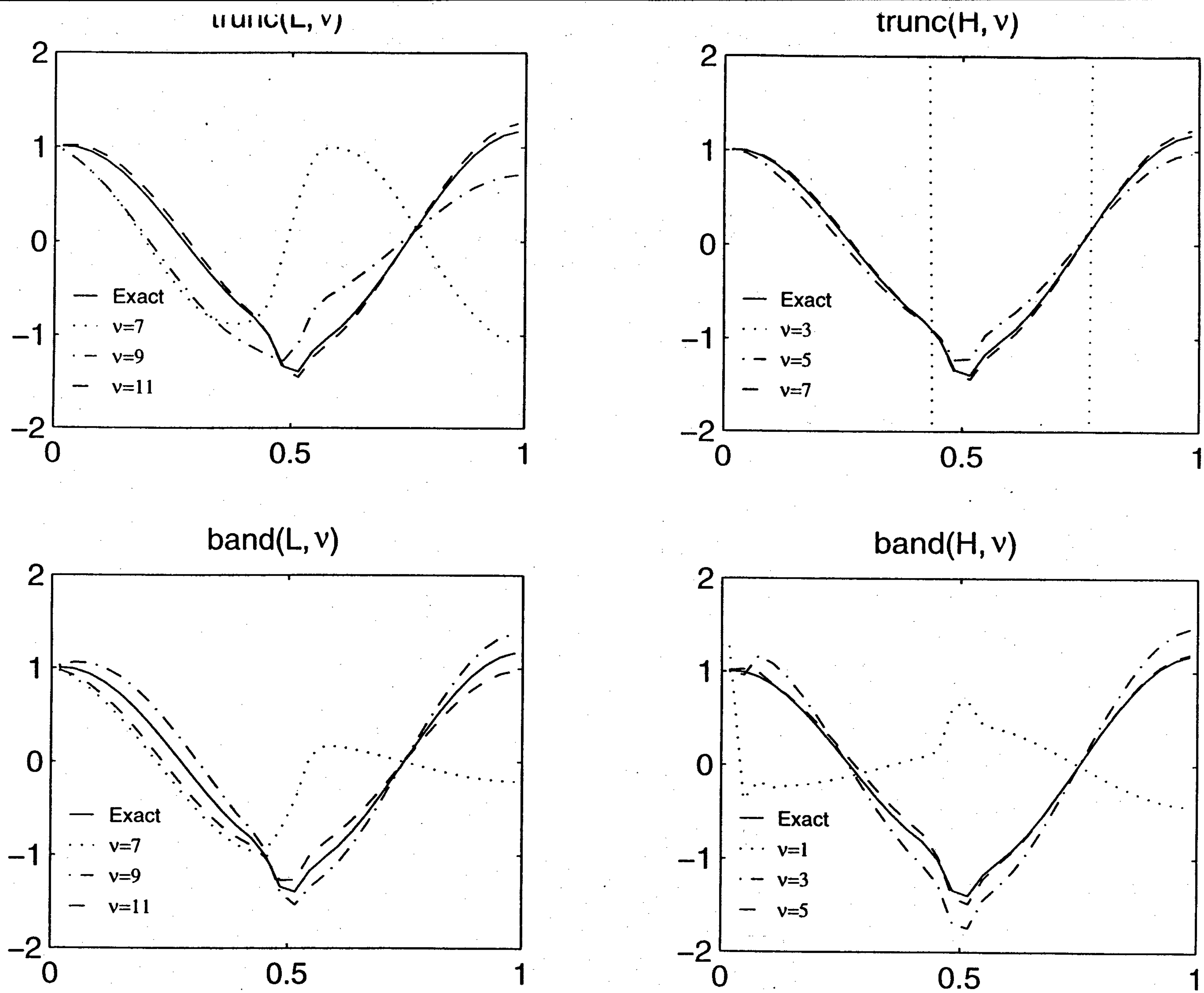

trunc(L, ν)
Exact
ν=7
ν=9
ν=11
trunc(H, ν)
Exact
ν=3
ν=5
ν=7
band(L, ν)
Exact
ν=7
ν=9
ν=11
band(H, ν)
Exact
ν=1
ν=3
ν=5

Figure 1

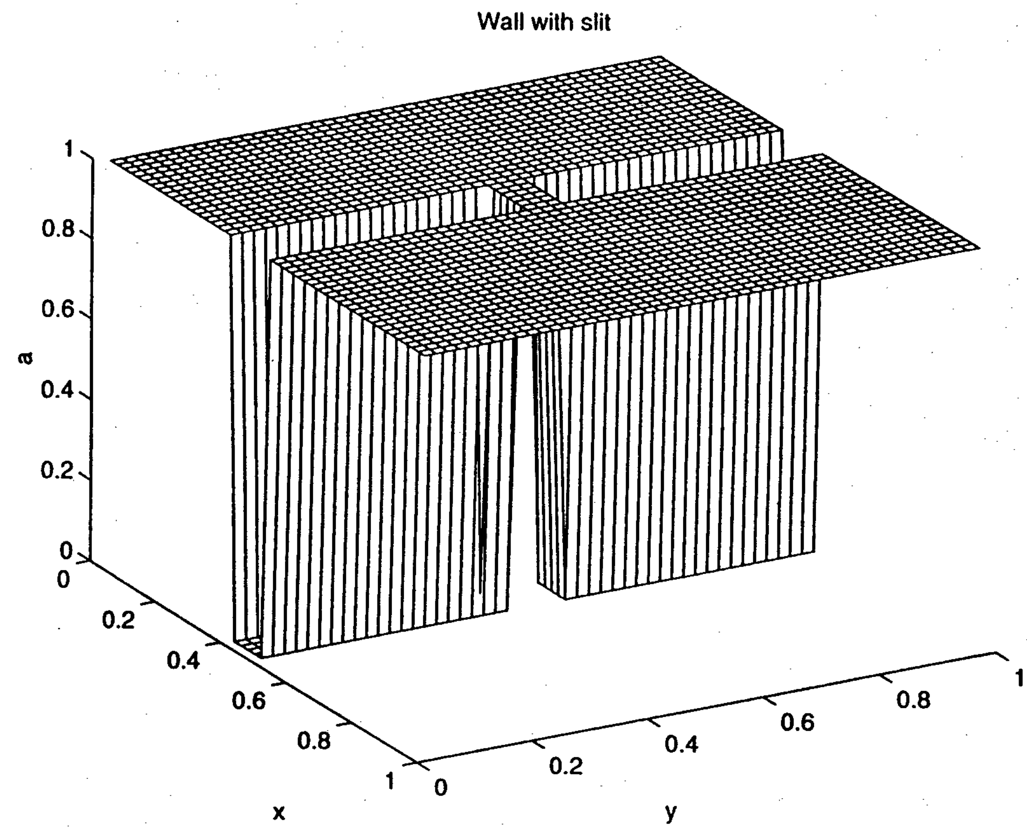

Figure 2

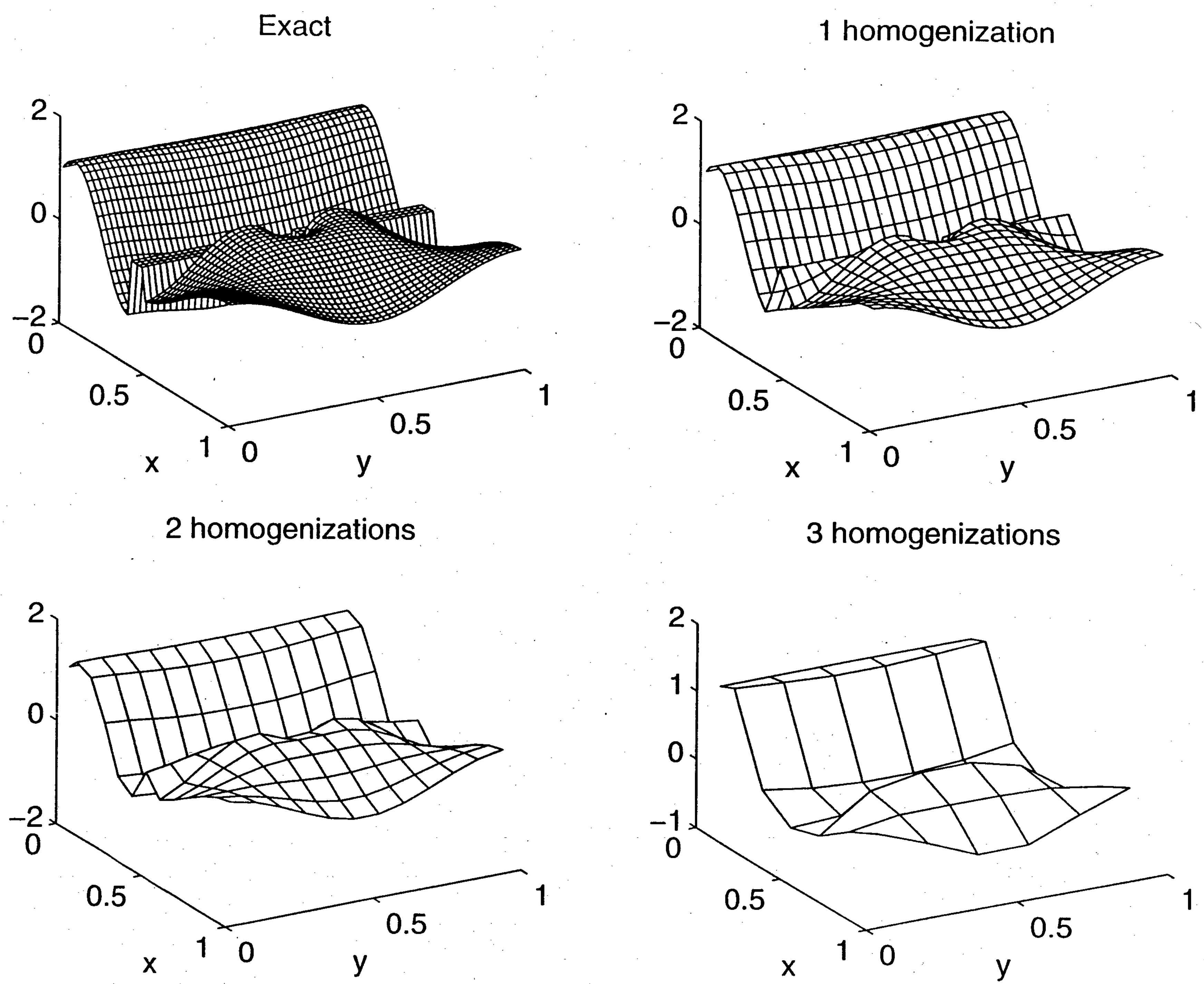
Exact
1 homogenization
2 homogenizations
3 homogenizations
x
y
0
0.5
1
2
1
0
−1
−2

Figure 3

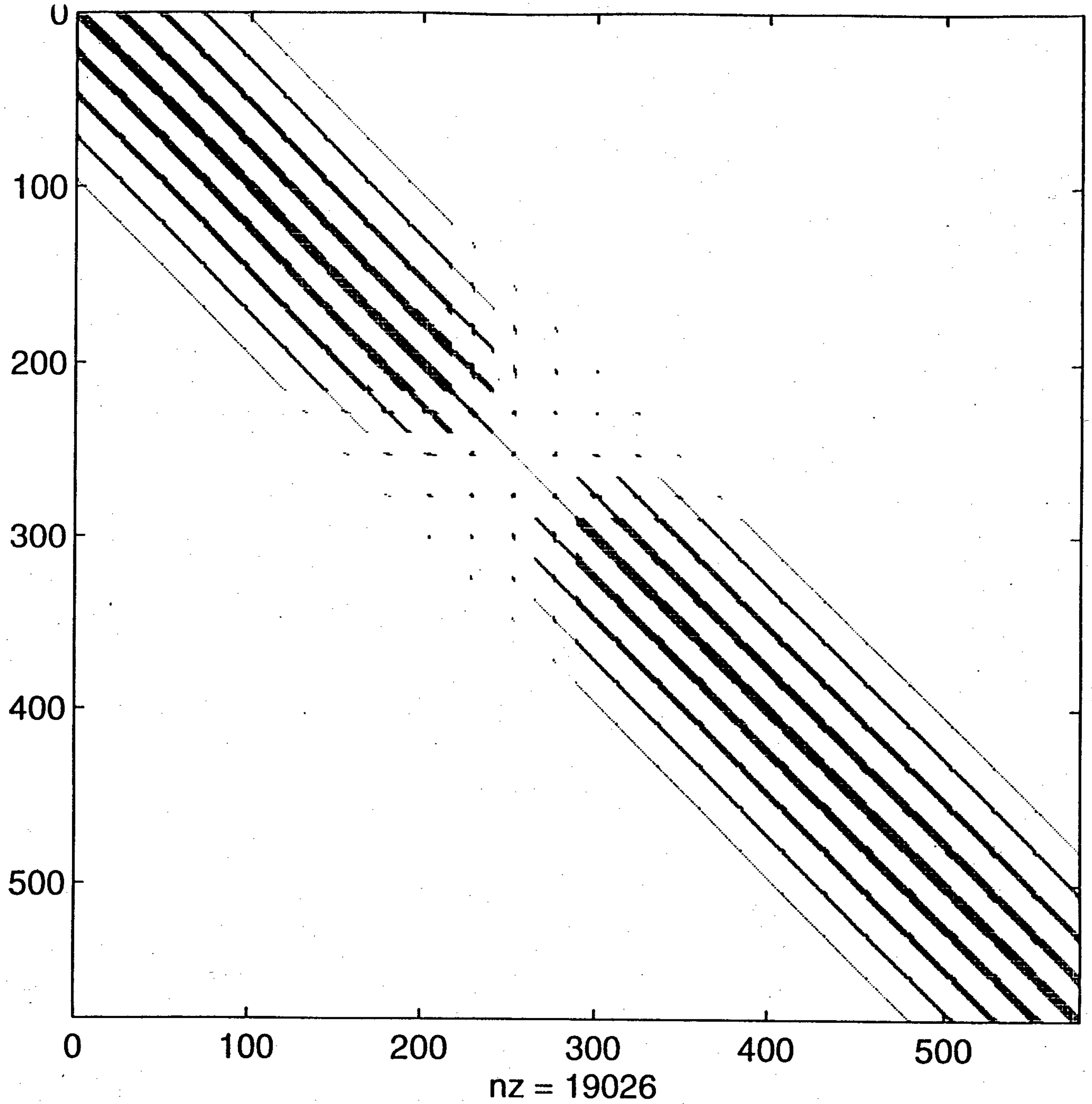

Figure 4

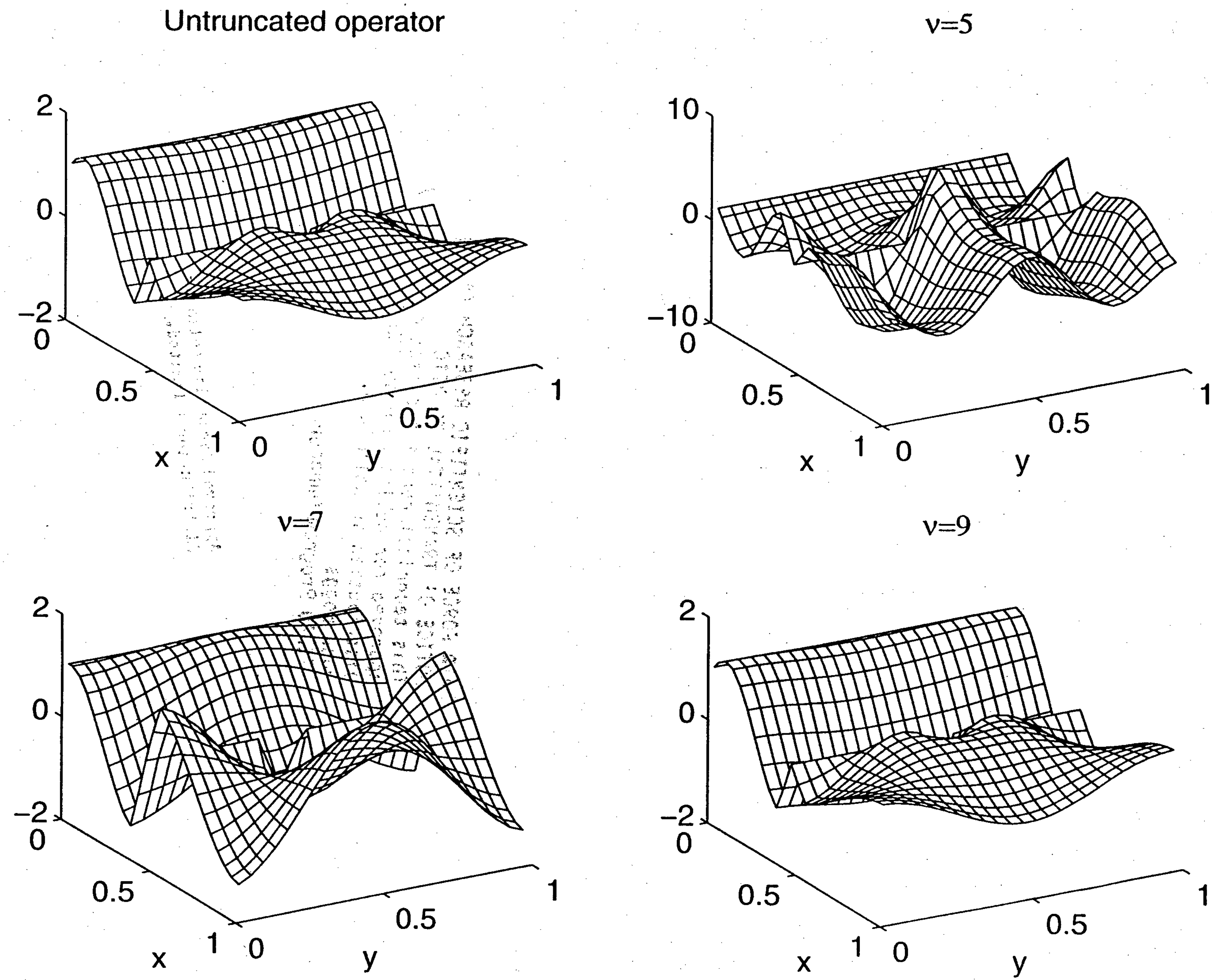

Figure 5